Palaeogeography, Palaeoclimatology, Palaeoecology 317–318 (2012) 32–40

Contents lists available at SciVerse ScienceDirect

Palaeogeography, Palaeoclimatology, Palaeoecology

journal homepage: www.elsevier.com/locate/palaeo

Negative $\delta^{18}O$–$\delta^{13}C$ relationship of pedogenic carbonate from northern China indicates a strong response of C_3/C_4 biomass to the seasonality of Asian monsoon precipitation

Shiling Yang *, Zhongli Ding, Xu Wang, Zihua Tang, Zhaoyan Gu

Key Laboratory of Cenozoic Geology and Environment, Institute of Geology and Geophysics, Chinese Academy of Sciences, Beijing 100029, China

ARTICLE INFO

Article history:
Received 17 July 2011
Received in revised form 3 December 2011
Accepted 10 December 2011
Available online 16 December 2011

Keywords:
Chinese loess
Pedogenic carbonate
East-Asian summer monsoon
Stable isotopes
C_3/C_4 vegetation
Precipitation seasonality

ABSTRACT

Evaluating how future climate changes may impact C_3/C_4 biomass in East Asia depends largely on the understanding of the relationship between past C_3/C_4 variations and Asian monsoon circulation. The glacial–interglacial variations in C_3/C_4 biomass have been readily ascribed to the summer monsoon. However, the internal processes governing the link of C_3/C_4 vegetation to the Asian monsoon have not been clearly described. Here we present isotopic results of pedogenic carbonate from northern China for the Holocene, the last and penultimate interglacial periods. Comparison of the observed and predicted $\delta^{18}O$ values of modern soil carbonate from gravelly soils suggests that pedogenic carbonate forms mainly in warm, rainy season. Carbonate nodules from the Chinese loess demonstrate a distinct negative $\delta^{18}O$–$\delta^{13}C$ relationship and a wider scatter of isotopic values in the southern Loess Plateau than in the northern part. By combining rainfall, $\delta^{18}O$ of precipitation and the peak of C_3 and C_4 plant metabolism, we develop a conceptual model to explain the isotopic signatures of the carbonate nodules. Our model shows that a narrowly-focused season of monsoon precipitation at a specific site produces low $\delta^{18}O$ values of soil water and simultaneously favors C_4 over C_3 plants. Our model further suggests that the scattered isotopic values of soil carbonate reflect a strong summer monsoon while the focused values indicate a weak summer monsoon. $\delta^{13}C$ values of soil carbonate indicate a striking pattern of northward-increasing C_4 vegetation for the last interglacial, while a flat spatial pattern is seen for the penultimate interglacial and the Holocene. It is inferred that the summer monsoon was stronger during the last interglacial than during the penultimate interglacial and the Holocene, leading to a northward displacement of C_3 forest ecosystems into the southern Loess Plateau. In addition, an in-phase relationship between intra-nodule $\delta^{13}C$ and $\delta^{18}O$ values suggests a strong and possibly rapid response of C_3/C_4 biomass to the seasonality of Asian monsoon precipitation. In this context, if the last interglacial period (MIS 5) is taken as an analog for the projected near future, then C_3 plants may be favored in the south while C_4 plants may be efficient in the north.

1. Introduction

Plants use two principal biosynthetic pathways to fix carbon, the C_3 and C_4 cycles. C_3 plants have $\delta^{13}C$ values ranging from −22‰ to −34‰, and C_4 plants from −10‰ to −14‰ (Deines, 1980; O'Leary, 1988; Farquhar et al., 1989). Recently, many modeling studies have projected increased monsoon precipitation in East Asia under CO_2-induced global warming (e.g., Kimoto, 2005; Kripalani et al., 2007; Sun and Ding, 2010). In this scenario, the regional C_3/C_4 biomass is expected to change, which would impact the global carbon cycle (Still et al., 2003) and agricultural production (Leakey, 2009; Liu et al., 2010) in densely populated East Asia. As such, it is important to evaluate how future monsoon changes may impact regional C_3/C_4 biomass.

Past C_3/C_4 vegetation records from the Chinese Loess Plateau may provide valuable clues on the composition of future terrestrial ecosystems. Generally, lower atmospheric pCO_2, higher temperature and enhanced summer precipitation favor C_4 over C_3 plants (Sage et al., 1999). Recent studies have shown that C_4 plants declined in glacials and increased in interglacials, with its cause being ascribed to temperature (Gu et al., 2003; Zhang et al., 2003) or both temperature and precipitation seasonality (Vidic and Montañez, 2004; An et al., 2005; Liu et al., 2005). Whichever the dominant cause, it is clear that the C_3/C_4 variations in East Asia are closely connected to the monsoon climate. However, the internal processes linking the C_3/C_4 changes to the East-Asian monsoon system have not been clearly described. This is because C_3/C_4 biomass and the monsoon signal are recorded in different geologic archives, the former reconstructed from the $\delta^{13}C$ value of soil organic matter, and the latter from

* Corresponding author at: Key Laboratory of Cenozoic Geology and Environment, Institute of Geology and Geophysics, Chinese Academy of Sciences, 19 BeiTuChengXi Road, Beijing 100029, China. Tel.: +86 10 82998526; fax: +86 10 62010846.
E-mail address: yangsl@mail.iggcas.ac.cn (S. Yang).

0031-0182/$ – see front matter © 2011 Elsevier B.V. All rights reserved.
doi:10.1016/j.palaeo.2011.12.007

paleoclimate proxies such as magnetic susceptibility (Gu et al., 2003; Zhang et al., 2003; Vidic and Montañez, 2004; Liu et al., 2005).

Warm-season precipitation is a defining feature of the summer monsoon circulation. The $\delta^{18}O$ value of precipitation ($\delta^{18}O_p$) integrates all aspects of atmospheric transport from source to sink and shows a strong seasonal variation in response to the monsoon system (Rozanski et al., 1993; Araguás-Araguás et al., 1998; Johnson and Ingram, 2004; Vuille et al., 2005). Thus $\delta^{18}O_p$ is ultimately a recorder of the summer monsoon system. Pedogenic carbonate nodules are abundant at the base of interglacial paleosols within Chinese loess (Liu, 1985). Their carbon ($\delta^{13}C_{cc}$) and oxygen isotope ($\delta^{18}O_{cc}$) composition record the proportion of C_3/C_4 vegetation and the $\delta^{18}O$ value of soil water (ultimately derived from meteoric water), respectively (Wang and Zheng, 1989; Han et al., 1997; Wang and Follmer, 1998; Ding and Yang, 2000). Therefore, investigation of $\delta^{18}O$–$\delta^{13}C$ relationship of carbonate nodules may have great potential to explore the monsoon-C_3/C_4 vegetation linkage, which is central to the prediction of C_3/C_4 response to the projected climate change.

In this study, we first investigate the $\delta^{18}O_{cc}$ values in modern soils at two sites around the Loess Plateau, where the continuous $\delta^{18}O_p$ data are available from the Global Network of Isotopes in Precipitation (GNIP) (IAEA/WMO, 2006), in order to identify the season of carbonate formation. We then present the temporal and spatial isotopic results of interglacial carbonate nodules from Chinese loess, the $\delta^{18}O$–$\delta^{13}C$ relationship, and examine the causes of these patterns.

2. Setting, materials, and methods

Fifty-nine samples of modern soil carbonate were taken from gravelly soils on river terraces at Baotou and Yinchuan (Fig. 1A). Gravels in these deposits are dominated by dioritic, amphibolitic and some metasedimentary rocks. Carbonate clasts are rare to absent, thus insuring against detrital contamination of our secondary carbonate samples by local bedrock. No surface soil horizons (A horizons) show visible darkening from organic matter. The soil carbonate is characterized by thin, discontinuous to semi-continuous coatings on pebbles at both sites. According to the classification scheme of Gile et al. (1966), the development of carbonate is assigned to Stage I to weak Stage II and is assumed to require 10^3 to 10^4 years.

Carbonate nodules, a common form of pedogenic carbonate in the Chinese loess, were collected from 22 loess sections (Fig. 1A). These sites lie along two approximately north–south loess transects, stretching from Hongde to Yangling and Hengshan to Lantian. At present, the mean annual precipitation and temperature are ~400 mm and ~8.5 °C in the north, the values in the south being ~600 mm and ~13.5 °C. Most sections consist of the loess (L)–soil (S) sequence S0, L1, S1, L2, and S2 (Fig. 2), although over 30 loess–soil couplets have been identified in complete Chinese loess sequences (Rutter et al., 1991; Ding et al., 1993, 1999b; Yang and Ding, 2010). The loess units L1 and L2 were deposited during the last and penultimate glacial periods, respectively. Both L1 and L2 are yellowish in color and massive in structure. Previous studies (Kukla, 1987; Ding et al., 2002; Lu et al., 2007) have shown that L1 is correlated with marine isotope stages (MIS) 2 to 4, and the L2 loess unit with MIS 6. The Holocene soil, S0, is dark in color because of its relatively high organic matter content, and has been partly or totally eroded, or disturbed by agricultural activities at most sites. The soil units S1 and S2 developed in the last and penultimate interglacial periods and correlate with MIS 5 and 7, respectively (Kukla, 1987; Ding et al., 2002; Lu et al., 2007). Both of the soils are brownish or reddish in color, and have an A–B–C horizon sequence. Soil unit S2 is composed of two soils (S2-1 and S2-2) and a thin intervening loess horizon. Based on a stacked orbital timescale of Chinese loess (Ding et al., 2002), the soil units S0, S1, S2-1 and S2-2 formed in the periods 11–0 ka, 128–73 ka, 219–190 ka, and 245–234 ka, respectively. Details of site locations and lithostratigraphy are given in Yang and Ding (2008).

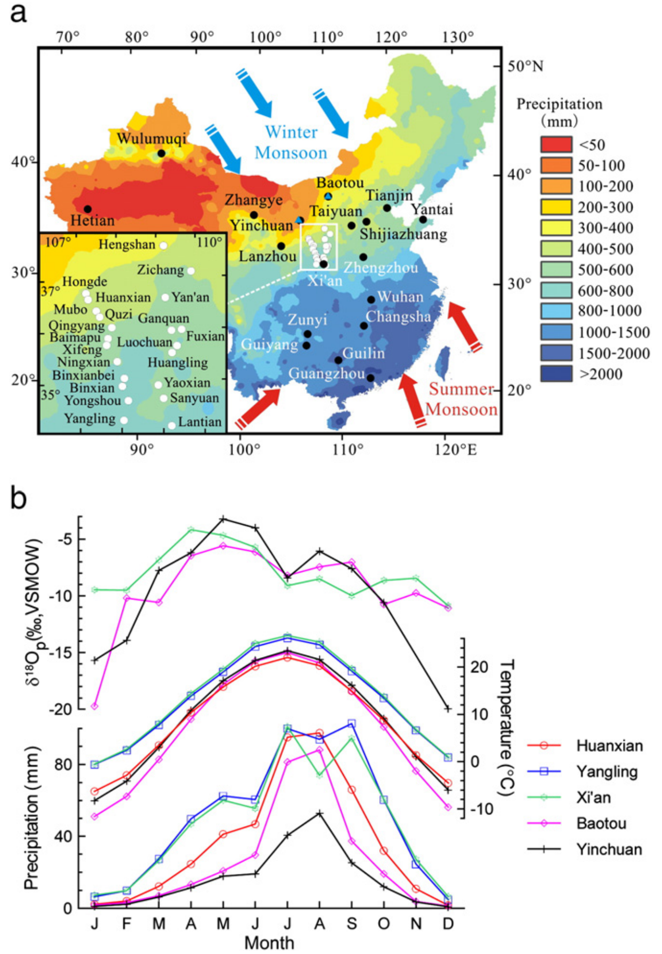

Fig. 1. A) Mean annual precipitation of China. The rainfall data come from the Data Center for Resources and Environmental Sciences, CAS (RESDC). GNIP sites (black circles), loess sites (white circles), and modern soil sites (blue triangles) are indicated. The blue and red arrows indicate the East-Asian winter and summer monsoon winds, respectively. B) Monthly mean data for weighted $\delta^{18}O$ of precipitation ($\delta^{18}O_p$), temperature, and precipitation for selected sites in and around the Loess Plateau. Precipitation and temperature data are averaged values over 51 years (1951–2001) and come from China Meteorological Data Sharing Service System. The mean weighted $\delta^{18}O_p$ values were computed from the GNIP $\delta^{18}O_p$ data (IAEA/WMO, 2006) weighted by precipitation amount.

Carbonate nodules, with grayish color and sub-spherical or irregular shape, are commonly found at the base of paleosols (Bk horizons) but are rare within loess units. The abundance of detrital carbonate in glacial loess units and scarcity in interglacial soils indicate formation of carbonate nodules during interglacial (soil-forming) stages (Liu, 1985; Kukla, 1987; Liu and Ding, 1998). Generally, nodules at the base of the Holocene soil (S0) are sporadic and small (<1.5 cm) and can be found only in the central and southern Loess Plateau. For the soil units S1, S2-1 and S2-2, nodule sizes range from a few centimeters in the north to over 10 cm in the south. We took 1 to 6 nodules from each carbonate nodule layer, with a total of 142 samples collected.

Carbonate nodules were broken to reveal their internal structure and to avoid analysis of any nonpedogenic spar. In order to investigate the temporal isotopic variations, micritic carbonate was microsampled under a binocular microscope with a 0.5 mm drill bit at 1–1.5 mm intervals along an interior cross-section of a large nodule (11.4 cm across; Fig. 4A), taken from the base of S1 at Ganquan (Figs. 1A and 2). For the study of spatial isotopic variations, the micrite from the inner part (~2 g) was ground to powder. Samples were heated under vacuum at 190 °C for 2 h to remove organic compounds prior to isotopic analysis. Some samples were processed using

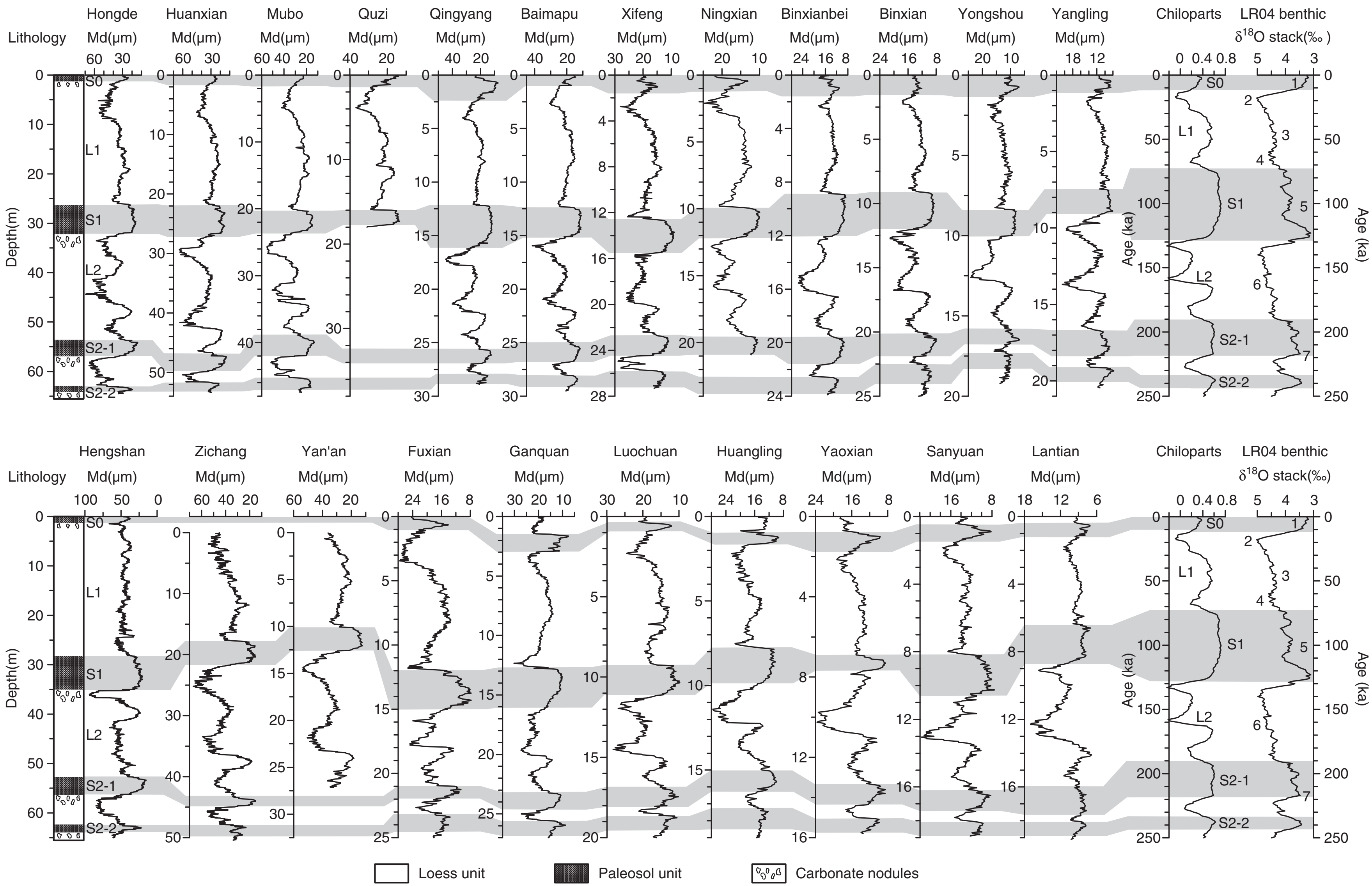

Fig. 2. Stratigraphic column and median grain size (Md) for the Hongde–Yangling and Hengshan–Lantian transects, and correlation with a stacked benthic $\delta^{18}O$ record (Lisiecki and Raymo, 2005) and a stacked Chinese loess particle size record (Chiloparts) (Ding et al., 2002). Interglacial paleosols (shaded zones) are characterized consistently by finer particle sizes, compared to the loess horizons above and below them. Grain size was measured with a SALD-3001 laser diffraction particle analyzer. The particle analytical procedures were as detailed by Ding et al. (1999a).

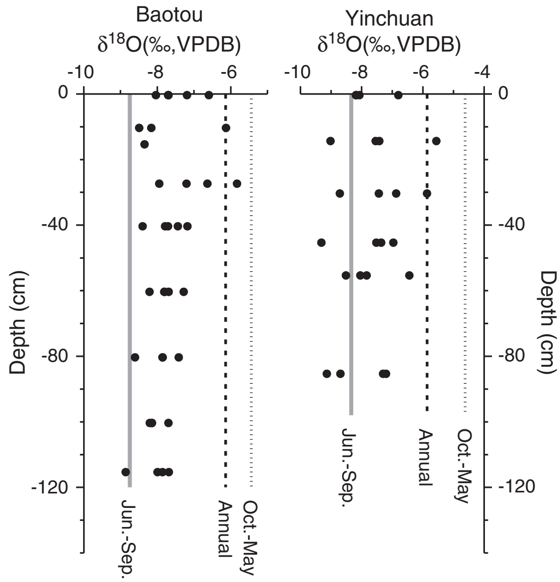

Fig. 3. Measured $\delta^{18}O$ (VPDB) of modern soil carbonate (black circles) versus soil depth from Baotou and Yinchuan, compared to the predicted $\delta^{18}O$ values of pedogenic carbonate calculated using mean weighted $\delta^{18}O_p$ and temperature of annual period (dashed lines), warm, rainy season (June to September, gray lines), and cold, dry season (October to May, dotted lines). For calculations, see Table 1.

an automated sample preparation device (Kiel III) attached directly to a Finnigan MAT 252 mass spectrometer at the University of Arizona, and others measured using a GasBench II carbonate preparation device interfaced with a Finnigan MAT 253 mass spectrometer at the Institute of Geology and Geophysics, CAS. $\delta^{18}O$ and $\delta^{13}C$ values were normalized to NBS-19 based on internal lab standards. Repeat analyses ($n=17$) show that these procedures yield a precision of ±0.08‰ for $\delta^{13}C$ and ±0.11‰ for $\delta^{18}O$.

3. Isotopic results for modern soil carbonate and implications for the season of carbonate formation

The $\delta^{18}O_{cc}$ (VPDB) values in the modern soil at Baotou fall between −8.9‰ and −5.9‰, while the values from Yinchuan profile range from −9.4‰ to −5.6‰ (Fig. 3). The $\delta^{18}O_{cc}$ values from both profiles decrease slightly from the soil–air interface down to depths of 40–50 cm, and approach relatively constant values below 50 cm. This pattern is consistent with most results from modern soil profiles (Quade et al., 1989; Breecker et al., 2009), indicating the evaporation effect on $\delta^{18}O$ of shallow soil water.

The $\delta^{18}O_{cc}$ value is determined by the $\delta^{18}O_p$ value, soil temperature, and the extent of evaporation of soil water prior to soil carbonate formation. By comparing to incipient pedogenic carbonate (Stage I–II) formed in climate conditions similar to today's, we can use the GNIP $\delta^{18}O_p$ (Fig. 1B) and modern surface temperature (Fig. 1B) to predict the mean $\delta^{18}O$ values for pedogenic carbonate at Baotou and Yinchuan, assuming the fractionation factor (α) between calcite and water of $1000\ln\alpha(\text{Calcite–H}_2\text{O})=18.03(10^3\,T^{-1})-32.42$, where T is in Kelvins (Kim and O'Neil, 1997). Considering significant seasonal fluctuations in temperature and precipitation (Fig. 1B), the predicted $\delta^{18}O_{cc}$ values are calculated for warm, rainy season (June to September), cold, dry season (October to May), and annual period (Table 1). Results show that the observed $\delta^{18}O_{cc}$ values below depth of 50 cm for both profiles fall closer to the predicted values for warm, rainy season than those for annual or cold, dry period (Fig. 3), indicating that pedogenic carbonate in northern China forms mainly in warm, rainy season.

The modern climate of East Asia is characterized by seasonal alternations of wet, warm summer monsoon and dry, cold winter monsoon (Fig. 1). The precipitation of pedogenic carbonate results from supersaturation of the soil solution with respect to bicarbonate, mainly associated with dewatering of soil by evapotranspiration (Quade et al., 1989) and/or decrease in soil pCO_2 (Breecker et al., 2009). Therefore, wet–dry cycles are required for pedogenic carbonate formation (Breecker et al., 2009). Chinese loess is composed mainly of loosely cemented silt (Liu, 1985; Liu and Ding, 1998), which allows rainwater to infiltrate quickly (Chen et al., 2008). The infiltrated rainwater mainly affects the moisture content in the near-surface soil (0 to 3 m depth) (Chen et al., 2008). Recent studies have shown that the temporal changes in soil moisture are closely related to the seasonal precipitation (Fu et al., 2003; Chen et al., 2008; Guan et al., 2009; Hu et al., 2010), and the soil moisture content decreases considerably during dry intervals between rain events (Chen et al., 2008). All these conditions favor the formation of soil carbonate in the season when the East-Asian summer monsoon prevails.

4. $\delta^{18}O$–$\delta^{13}C$ relationship for carbonate nodules from the Chinese loess

4.1. Intra-nodule (temporal) changes in $\delta^{13}C$ and $\delta^{18}O$ values

Microscopic examination of thin sections reveals a brown micritic ground mass for the large nodule, throughout which are dispersed detrital grains mainly of quartz and feldspar. These detrital grains, coarse silt in size, comprise ~10% of the nodule volume. The isotopic results (Fig. 4A, B) show significant intra-nodule (temporal) variations, with $\delta^{13}C_{cc}$ (VPDB) values ranging from −4.2‰ to −6.8‰ and $\delta^{18}O_{cc}$ (VPDB) values from −8.6‰ to −10.2‰. A striking feature is that $\delta^{18}O_{cc}$ values vary inversely (R = 0.85) with $\delta^{13}C_{cc}$ values (Fig. 4B, C). The growth center of the nodule is hard to find, as it displays neither growth layers (Fig. 4A) nor unambiguous symmetry of isotopic curves (Fig. 4B).

4.2. Spatial changes in $\delta^{13}C$ and $\delta^{18}O$ values

The isotopic values for the nodules from the transect sites show much larger variations than the intra-nodule changes (Fig. 4B, D, E),

Table 1
Calculations of the predicted $\delta^{18}O$ values for modern soil carbonate ($\delta^{18}O_{cc}$) at Baotou and Yinchuan.

Site	Period	Mean precipitation (mm)	Mean temperature (°C)	Mean weighted $\delta^{18}O_p$ (‰, VSMOW)	1000lnα	α	Predicted $\delta^{18}O_{cc}$ (‰, VSMOW)	Predicted $\delta^{18}O_{cc}$ (‰, VPDB)
Baotou (40.72°N, 109.81°E, 1101 m a.s.l.)	Annual	307	6.9	−7.66	31.9614	1.0325	24.57	−6.14
	June to September	237	20.0	−7.41	29.0843	1.0295	21.89	−8.75
	October to May	70	0.3	−8.50	33.5153	1.0341	25.30	−5.44
Yinchuan (38.52°N, 106.03°E, 1151 m a.s.l.)	Annual	193	8.8	−6.94	31.5275	1.0320	24.87	−5.86
	June to September	138	20.6	−6.87	28.9587	1.0294	22.31	−8.34
	October to May	55	2.8	−7.08	32.9179	1.0335	26.15	−4.62

We used mean weighted $\delta^{18}O$ values of local precipitation ($\delta^{18}O_p$) and local mean temperatures to predict the mean $\delta^{18}O$ values of pedogenic carbonate ($\delta^{18}O_{cc}$) for different periods. Monthly mean data for weighted $\delta^{18}O_p$, temperature, and precipitation are shown in Fig. 1B. The fractionation factor (α) between calcite and water was calculated using the equation of Kim and O'Neil (1997): $1000\ln\alpha(\text{Calcite–H}_2\text{O})=18.03(10^3\,T^{-1})-32.42$, where T is in kelvins ([K] = [°C] + 273.15). The predicted $\delta^{18}O_{cc}$ values were then obtained using the formula $\alpha=(1000+\delta^{18}O_{cc})/(1000+\delta^{18}O_p)$. The $\delta^{18}O_{cc}$ values expressed in VSMOW were converted to the VPDB scale using the relationship $\delta^{18}O_{VPDB}=0.97002\cdot\delta^{18}O_{VSMOW}-29.98‰$ (Coplen et al., 1983).

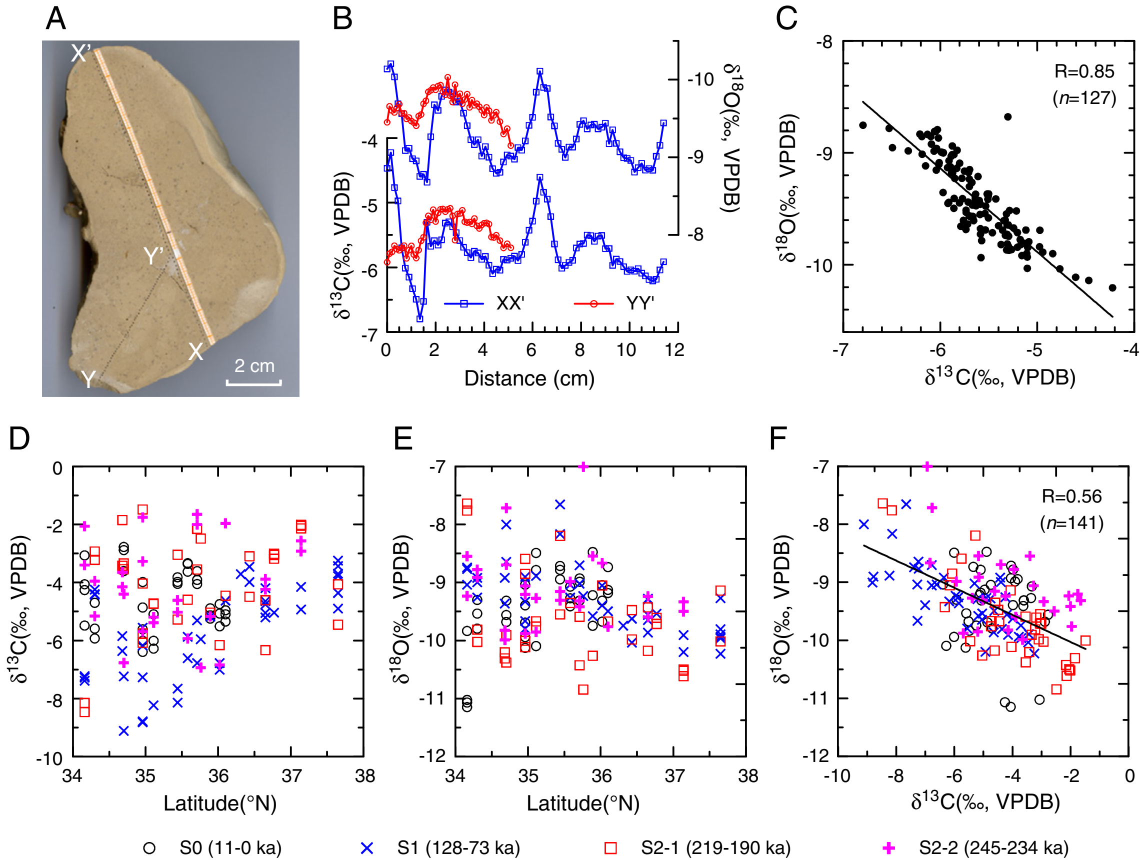

Fig. 4. $\delta^{18}O$ and $\delta^{13}C$ records (all in VPDB) for carbonate nodules from the Chinese loess. A) Cross-section (11.4 cm across) of a large nodule from the base of soil unit S1 (last interglacial) at Ganquan (Fig. 1A). B) Serial intra-nodule variations in $\delta^{18}O$ and $\delta^{13}C$ values along axes of XX′ and YY′ (A). C) $\delta^{18}O$ versus $\delta^{13}C$ values of serial samples from the large nodule. D) $\delta^{13}C$ values versus latitude for the nodules from the transect sites. E) $\delta^{18}O$ values versus latitude for the nodules from the transect sites. F) $\delta^{18}O$ versus $\delta^{13}C$ values of the nodules from the transect sites.

with the $\delta^{13}C_{cc}$ (VPDB) values ranging from −1.5‰ to −9.1‰ and the $\delta^{18}O_{cc}$ (VPDB) values from −7.0‰ to −11.1‰. During the last interglacial (S1), lower $\delta^{13}C_{cc}$ values occurred in the south (34–36°N) than in the north (36–38°N), showing a clear north–south gradient, while a flat spatial pattern is seen for the penultimate interglacial (S2-1 and S2-2) (Fig. 4D). For the Holocene (S0), the southern sites show slightly higher $\delta^{13}C_{cc}$ values than the central sites (Fig. 4D). The $\delta^{18}O_{cc}$ values are generally higher in the south (34–36°N) than in the north (36–38°N) for S1 and S2 times, while slightly lower $\delta^{18}O_{cc}$ values occur in the south than in the central part for S0 period (Fig. 4E). Both $\delta^{13}C_{cc}$ and $\delta^{18}O_{cc}$ values are more scattered in the south (34–36°N) than in the north (36–38°N). Again, a good inverse correlation ($R=0.56$) between $\delta^{13}C_{cc}$ and $\delta^{18}O_{cc}$ values is observed (Fig. 4F).

5. Mechanism for the negative $\delta^{18}O$–$\delta^{13}C$ relationship

Isotopic results of pedogenic nodules from the Chinese loess show a negative relationship between $\delta^{13}C_{cc}$ and $\delta^{18}O_{cc}$ values, i.e. the lower $\delta^{18}O_{cc}$ values the higher C_4 component. The three factors controlling the $\delta^{18}O_{cc}$ variations, namely the $\delta^{18}O_p$, soil temperature, and evaporation conditions, are discussed in detail as below.

If soil temperature were the major factor, then the 1.5‰ intra-nodule variations of $\delta^{18}O_{cc}$ (Fig. 4B) would have resulted from a ~7 °C temperature change (Kim and O'Neil, 1997). Assuming a maximum length of growth period (55 ka) for the large nodule from Ganquan (Fig. 4A), its isotopic data may have a time resolution of less than 1000–1500 years. Such an amplitude change in summer temperature at millennial to centennial scales is unlikely within relatively stable interglacial periods (Ding et al., 1999a). In addition, given the small spatial changes in both mean annual and summer $\delta^{18}O_p$ values over the Loess Plateau (Liu et al., 2008; Figs. 1B and 5B, C), the lower $\delta^{18}O_{cc}$ values in the north (36–38°N) for S2 and S1 times would indicate a higher temperature in the north than in the south (Kim and O'Neil, 1997), which is inconsistent with both the modern and past trends of increasing temperature southward (Yang and Ding, 2003). These lines of evidence show a minor role of temperature in the large variations of $\delta^{18}O_{cc}$ values (Fig. 4B, E).

Increased evaporation due to enhanced aridity would produce high $\delta^{18}O_{cc}$ values and low plant density, and vice versa. Thus a positive $\delta^{18}O_{cc}$–$\delta^{13}C_{cc}$ relationship is expected due to the significant contribution of ^{13}C-enriched atmospheric CO_2 to $\delta^{13}C_{cc}$ values, like the cases of soil carbonate from many of the world's deserts (Quade et al., 2007), rather than the observed negative one. Furthermore, a northward increase in aridity has been found for both glacials and interglacials (Yang and Ding, 2003). Thus the $\delta^{18}O_{cc}$ values are expected to be higher in the north than in the south. On the contrary, high $\delta^{18}O_{cc}$ values are observed in the south for S2 and S1 times (Fig. 4E). Thus evaporation may also play a minor role in the large variations of $\delta^{18}O_{cc}$ values (Fig. 4B, E).

Modern $\delta^{18}O_p$ values exhibit a large seasonal variation (Fig. 5) that is crucial for the understanding of the $\delta^{18}O_{cc}$–$\delta^{13}C_{cc}$ relationship. The $\delta^{18}O_p$ data show two features clearly (Fig. 5). (1) In the summer monsoon domain (Fig. 5C, D), low $\delta^{18}O_p$ values occur in summer due to amount effect, overshadowing the dependence of $\delta^{18}O_p$ on temperature (Araguás-Araguás et al., 1998; Johnson and Ingram, 2004; Vuille et al., 2005). This effect is visible as a distinct dip in $\delta^{18}O_p$ values during July to September in the monsoon-influenced southern sites (Fig. 5C, D). (2) The summertime “dip” decreases with distance inland, in the same direction that summer monsoon penetration diminishes (Figs. 1

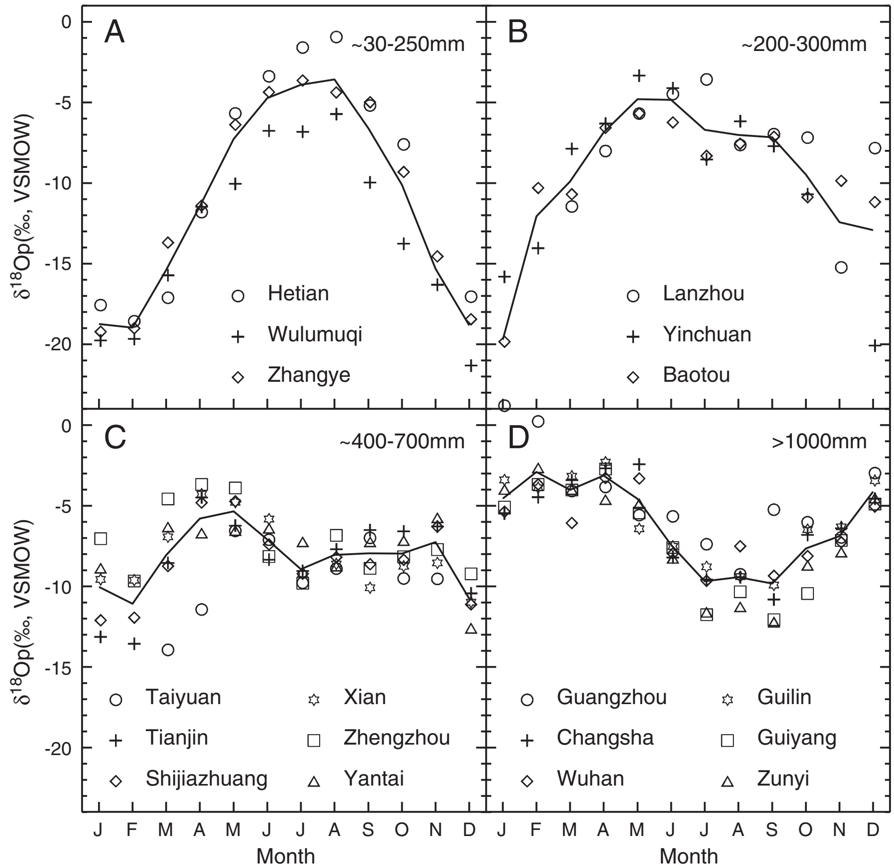

Fig. 5. Seasonal variations of weighted $\delta^{18}O_p$ (VSMOW) for selected GNIP sites in China. A) Sites outside the summer monsoon region. B) Sites in semi-arid areas. C) Sites in sub-humid areas. D) Sites in humid areas. The solid lines indicate the mean weighted $\delta^{18}O_p$ values of GNIP sites in each panel. Mean annual precipitation for the GNIP sites in each panel are shown in the top right corner. Rainfall data for calculating the weighted $\delta^{18}O_p$ come from China Meteorological Data Sharing Service System.

and 5). In this context, the summertime dip in $\delta^{18}O_p$ values is a distinctive characteristic of summer monsoon precipitation.

Although most of the annual precipitation occurs in summer on the Chinese Loess Plateau, the significant rainy period is shorter and more concentrated in the north than in the south (Fig. 1B). Two examples are shown (Fig. 1B): (1) the ratio of summer (June to September) to annual rainfall decreases from 70% at Huanxian to 59% at Yangling, and (2) at Huanxian, there are only three months (July to September) with over 50 mm rainfall, whereas at Yangling there are six months (May to October) with over 50 mm. Under these climate conditions, the duration of carbonate formation and plant growing season is longer in the south than in the north, as shown in a conceptual model (Fig. 6).

For a specific site, the peak of C_3 and C_4 plant metabolism differs seasonally (Ode et al., 1980), thus the pedogenic carbonate formed in summer may record the signals of relatively low $\delta^{18}O_p$ and high C_4 component (high $\delta^{13}C$ values) (Fig. 6), while that formed in spring and fall may document the signals of relatively high $\delta^{18}O_p$ and high C_3 component (low $\delta^{13}C$ values) (Fig. 6). These cases result in the negative $\delta^{18}O_{cc}$–$\delta^{13}C_{cc}$ relationship. For a spatial view of the Loess Plateau, the pedogenic carbonate in the south (Fig. 6B) may record the isotopic signatures of vegetation and precipitation for a longer period than that in the north (Fig. 6A), leading to a wide scatter of isotopic values in the south. It should be noted that the lowest $\delta^{18}O_p$ values on the Loess Plateau occur in winter (Fig. 5B, C), however, the extremely low rainfall (<10 mm/month) can hardly cause the dissolution of carbonate minerals, much less the carbonate reprecipitation (Royer, 1999).

A negative $\delta^{18}O$–$\delta^{13}C$ relationship has also been found in horse tooth enamel from northwestern China for the Pleistocene, and was attributed to the summer monsoon activity (Biasatti et al., 2010). These observations strongly support our findings. As pedogenic carbonate forms mainly in summer, a period of C_4 plant growth (Fig. 6), its $\delta^{13}C$ value is biased toward a C_4 signal. Therefore the C_4 biomass estimated from $\delta^{13}C_{cc}$ values should be regarded as upper limits. The negative $\delta^{18}O_{cc}$–$\delta^{13}C_{cc}$ relationship suggests that a narrowly-focused season of monsoon precipitation at a specific site produces low $\delta^{18}O_p$ values and simultaneously favors C_4 over C_3 plants and vice versa. Today, the summer monsoon simultaneously becomes weaker and more focused from southeast to northwest (Fig. 1B). It follows from this that, within the marginal zone of the summer monsoon, the scattered isotopic values of soil carbonate reflect a relatively strong summer monsoon (Fig. 6B) while the focused values indicate a weak summer monsoon (Fig. 6A). In contrast to the soil organic matter that records long-term annual average of the floral biomass (Wang and Follmer, 1998), the pedogenic carbonate is therefore a robust tool to reconstruct the seasonality of Asian monsoon precipitation.

6. Latitudinal patterns of C_3/C_4 vegetation and summer monsoon strength for different interglacial periods

The modern distribution of C_3/C_4 plants in East Asia is closely related to summer monsoon intensity. From southeast to northwest of China, the vegetation changes from broadleaf deciduous forest in a strong monsoon area to steppe in an intermediate monsoon region, and then to desert steppe in a weak monsoon area (Hou, 1983; Passey et al., 2009). Carbon isotope composition of soil organic matter (Rao et al., 2008) and phytoliths (Lü et al., 2000) from surface soils reveal a C_4 maximum zone between 31°N and 40°N in east China. At present, the Chinese Loess Plateau is characterized by mixed C_3–C_4 steppe, with C_3 forest dominant to the south of the Plateau, and C_3

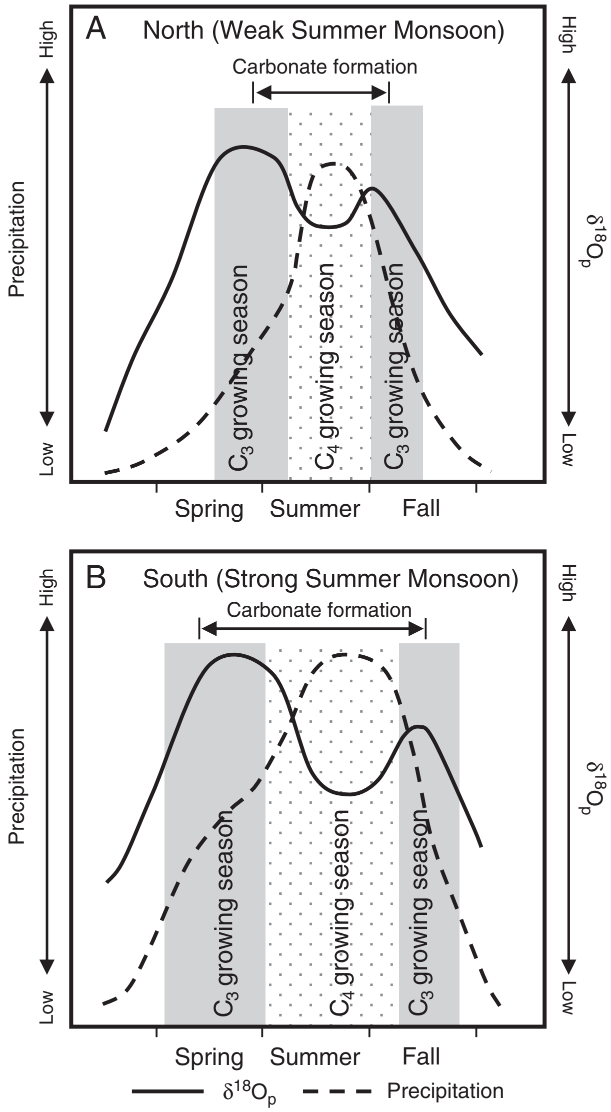

Fig. 6. Conceptual model for seasonal-bias in the formation of pedogenic carbonate on the Chinese Loess Plateau. A) Pedogenic carbonate formation on the northern Loess Plateau (a region of weak summer monsoon). B) Pedogenic carbonate formation on the southern Loess Plateau (a region of relatively strong summer monsoon). The solid and dashed lines indicate monthly mean $\delta^{18}O$ of precipitation ($\delta^{18}O_p$) and rainfall, respectively. The shaded and dotted areas indicate C_3 and C_4 growing seasons, respectively. Note the higher rainfall, longer rainy season, and longer growing seasons in the south (B) than in the north (A).

desert steppe dominant to the north of the Plateau (Hou, 1983; Wang, 2003; Passey et al., 2009). Passey et al. (2009) developed a conceptual model on the relationship between paleobiome transition and summer monsoon strength. According to this model, a stronger summer monsoon than at present would lead to a northward displacement of C_3 forest–C_3+C_4 steppe–C_3 desert steppe transition, thus dampening or even reversing the current pattern of southward-increasing C_4 vegetation.

Our $\delta^{13}C_{cc}$ values from the Holocene soil (S0) show a pattern of slightly southward-increasing C_4 vegetation (Fig. 4D), consistent with the $\delta^{13}C$ records of soil organic matter (Gu et al., 2003; Liu et al., 2005). For the last interglacial (S1), the $\delta^{13}C_{cc}$ values indicate a striking pattern of northward-increasing C_4 vegetation, while a flat gradient of C_3/C_4 biomass is seen for the penultimate interglacial (S2-1 and S2-2) (Fig. 4D). It follows that the East-Asian summer monsoon is stronger during the last interglacial than during the penultimate interglacial and the Holocene.

Two lines of evidence support the strengthened summer monsoon during the last interglacial. First, the soil unit S1 has stronger pedogenic characteristics than S2 and S0, as indicated by its better developed soil structure (Rutter et al., 1991; Ding et al., 1999b). Second, pollen studies have shown that forest (C_3 ecosystems) occurred in the southernmost Loess Plateau during a short interval of the last interglacial (S1) (Sun et al., 1997), which well explains the northward increase in the $\delta^{13}C_{cc}$ values. The strengthened summer monsoon during the last interglacial (MIS 5) may be causally related to a decrease in global ice volume, as indicated by the sea level records (Siddall et al., 2007). The enhanced summer monsoon resulted in high precipitation and long rainy season during the last interglacial, which favored C_3 forest ecosystems at least on the southernmost Loess Plateau. In this context, if the last interglacial stage (MIS 5) is referenced as an analog for near-future warming (Kopp et al., 2009), the C_3 crops (e.g., wheat and soybeans) may be favored in the south while the C_4 crops (e.g., maize, millet, and sorghum) may be efficient in the north.

7. A rapid response of C_3/C_4 vegetation to the summer monsoon variations?

In most arid and semi-arid ecosystems, plant productivity responds instantaneously or quasi-instantaneously to pulses of precipitation, which is known as the 'Pulse-Reserve' Paradigm (Noy-Meir, 1973; Reynolds et al., 2004). According to this paradigm, pulses of precipitation trigger primary production and result in reserves of carbon and energy that accumulate in seeds, storage organs, etc., and these reserves are able to persist through dry interpulse periods.

To date, there are no precise age constraints for carbonate nodules owing to the lack of reliable dating methods. As mentioned earlier, the isotopic data of the large nodule (Fig. 4A, B) may have a time resolution of less than 1000–1500 years. Since the processes of soil carbonate formation are similar to those of stalagmite formation, the in-phase relationship between intra-nodule $\delta^{18}O$ and $\delta^{13}C$ values (Fig. 4B) suggests a strong and possibly rapid response of C_3/C_4 biomass to the seasonality of Asian monsoon precipitation on the Loess Plateau. This contention is supported by the finding of Warne et al. (2010) that the summer monsoonal rains in the Chihuahuan desert trigger a pulse of C_4 plant production.

8. Conclusions

Isotopic study of modern soil carbonate shows that pedogenic carbonate in northern China forms mainly in warm, rainy season, when the East-Asian summer monsoon prevails. Carbonate nodules from the Chinese loess show a distinct negative $\delta^{18}O$–$\delta^{13}C$ relationship and a wider scatter of isotopic values in the southern Loess Plateau than in the northern part. In East Asia, $\delta^{18}O$ values of modern meteoric water decrease during summer monsoon rainy season and this summertime dip is a distinctive characteristic of summer monsoon precipitation. By combining rainfall, $\delta^{18}O$ of precipitation and seasonal difference in the peak of C_3 and C_4 plant metabolism, we develop a model to explain the isotopic signatures of the carbonate nodules. Our model suggests that a narrowly-focused season of monsoon precipitation at a specific site produces low $\delta^{18}O_p$ values and simultaneously favors C_4 over C_3 plants, leading to a negative $\delta^{18}O_{cc}$–$\delta^{13}C_{cc}$ relationship. Our model further indicates that, within the marginal zone of the summer monsoon, the scattered isotopic values of soil carbonate reflect a relatively strong summer monsoon while the focused values indicate a weak summer monsoon. The pedogenic carbonate is therefore a robust tool to reconstruct the seasonality of Asian monsoon precipitation.

The $\delta^{13}C_{cc}$ records show a striking pattern of northward-increasing C_4 vegetation for the last interglacial (S1), while a relatively flat spatial gradient of C_3/C_4 biomass is seen for the penultimate interglacial (S2-1 and S2-2) and the Holocene (S0). We infer a stronger summer monsoon (higher precipitation and longer rainy season) during S1 time than during S2 and S0 times, which caused a northward displacement of C_3 forest ecosystems into the southern Loess Plateau during the last interglacial. In addition, the intra-nodule isotopic data show an in-phase relationship of $\delta^{18}O$ and $\delta^{13}C$ values, suggesting a strong and possibly rapid response of C_3/C_4 biomass to the seasonality of Asian monsoon precipitation on the Chinese Loess Plateau. In this context, if the last interglacial is used as an analog for near-future warming, C_3 plants may be favored in the south while C_4 plants may be efficient in the north.

Acknowledgments

This study is supported by the National Basic Research Program of China (973 Program) (Grant No. 2010CB950204), the Knowledge Innovation Program of the Chinese Academy of Sciences (Grant No. KZCX2-YW-Q1-03), the Strategic Priority Research Program of the Chinese Academy of Sciences (Grant No. XDA05120204), and the National Natural Science Foundation of China (Grant No. 40972228). We thank J.M. Sun and P. Luo for discussions, H.G. Sun for help with figure preparation, and Q. Qian, H.C. Jiang, B.G. Cai, G.Q. Chu, and Y.G. Ma for field and lab assistance. We are greatly indebted to J.T. Han, J. Quade, D. Breecker, Editor A.P. Kershaw, and three anonymous reviewers for their constructive comments that improved the manuscript.

References

An, Z., Huang, Y., Liu, W., Guo, Z., Clemens, S., Li, L., Prell, W., Ning, Y., Cai, Y., Zhou, W., Lin, B., Zhang, Q., Cao, Y., Qiang, X., Chang, H., Wu, Z., 2005. Multiple expansions of C_4 plant biomass in East Asia since 7 Ma coupled with strengthened monsoon circulation. Geology 33, 705–708.

Araguás-Araguás, L., Froehlich, K., Rozanski, K., 1998. Stable isotope composition of precipitation over southeast Asia. Journal of Geophysical Research 103, 28721–28742.

Biasatti, D., Wang, Y., Deng, T., 2010. Strengthening of the East Asian summer monsoon revealed by a shift in seasonal patterns in diet and climate after 2–3 Ma in northwest China. Palaeogeography, Palaeoclimatology, Palaeoecology 297, 12–25.

Breecker, D.O., Sharp, Z.D., McFadden, L.D., 2009. Seasonal bias in the formation and stable isotopic composition of pedogenic carbonate in modern soils from central New Mexico, USA. Geological Society of America Bulletin 121, 630–640.

Chen, H., Shao, M., Li, Y., 2008. The characteristics of soil water cycle and water balance on steep grassland under natural and simulated rainfall conditions in the Loess Plateau of China. Journal of Hydrology 360, 242–251.

Coplen, T.B., Kendall, C., Hopple, J., 1983. Comparison of stable isotope reference samples. Nature 302, 236–238.

Deines, P., 1980. The isotopic composition of reduced organic carbon. In: Fritz, P., Fontes, J.C. (Eds.), Handbook of Environmental Isotope Geochemistry I, The Terrestrial Environment. Elsevier, Amsterdam, pp. 329–406.

Ding, Z.L., Yang, S.L., 2000. C_3/C_4 vegetation evolution over the last 7.0 Myr in the Chinese Loess Plateau: evidence from pedogenic carbonate $\delta^{13}C$. Palaeogeography, Palaeoclimatology, Palaeoecology 160, 291–299.

Ding, Z.L., Rutter, N., Liu, T.S., 1993. Pedostratigraphy of Chinese loess deposits and climatic cycles in the last 2.5 Myr. Catena 20, 73–91.

Ding, Z.L., Ren, J.Z., Yang, S.L., Liu, T.S., 1999a. Climate instability during the penultimate glaciation: evidence from two high-resolution loess records, China. Journal of Geophysical Research 104, 20123–20132.

Ding, Z.L., Xiong, S.F., Sun, J.M., Yang, S.L., Gu, Z.Y., Liu, T.S., 1999b. Pedostratigraphy and paleomagnetism of a ~7.0 Ma eolian loess–red clay sequence at Lingtai, Loess Plateau, north-central China and the implications for paleomonsoon evolution. Palaeogeography, Palaeoclimatology, Palaeoecology 152, 49–66.

Ding, Z.L., Derbyshire, E., Yang, S.L., Yu, Z.W., Xiong, S.F., Liu, T.S., 2002. Stacked 2.6-Ma grain size record from the Chinese loess based on five sections and correlation with the deep-sea $\delta^{18}O$ record. Paleoceanography 17, 1033. doi:10.1029/2001PA000725.

Farquhar, G.D., Ehleringer, J.R., Hubrick, K.T., 1989. Carbon isotopic discrimination and photosynthesis. Annual Review of Plant Physiology and Plant Molecular Biology 40, 503–537.

Fu, B., Wang, J., Chen, L., Qiu, Y., 2003. The effects of land use on soil moisture variation in the Danangou catchment of the Loess Plateau, China. Catena 54, 197–213.

Gile, L.H., Peterson, F.F., Grossman, R.B., 1966. Morphological and genetic sequences of carbonate accumulation in desert soils. Soil Science 101, 347–360.

Gu, Z., Liu, Q., Xu, B., Han, J., Yang, S., Ding, Z., Liu, T., 2003. Climate as the dominant control on C_3 and C_4 plant abundance in the Loess Plateau: organic carbon isotope evidence from the last glacial–interglacial loess–soil sequences. Chinese Science Bulletin 48, 1271–1276.

Guan, X.D., Huang, J.P., Guo, N., Bi, J.R., Wang, G.Y., 2009. Variability of soil moisture and its relationship with surface albedo and soil thermal parameters over the Loess Plateau. Advances in Atmospheric Sciences 26, 692–700.

Han, J., Keppens, E., Liu, T., Paepe, R., Jiang, W., 1997. Stable isotope composition of the carbonate concretion in loess and climate change. Quaternary International 37, 37–43.

Hou, H.Y., 1983. Vegetation of China with reference to its geographical distribution. Annals of the Missouri Botanical Garden 70, 509–549.

Hu, W., Shao, M., Han, F., Reichardt, K., Tan, J., 2010. Watershed scale temporal stability of soil water content. Geoderma 158, 181–198.

IAEA/WMO, 2006. Global network of isotopes in precipitation. The GNIP Database. http://www.iaea.org/water. Downloaded 13-June-2010.

Johnson, K.R., Ingram, B.L., 2004. Spatial and temporal variability in the stable isotope systematics of modern precipitation in China: implications for paleoclimate reconstructions. Earth and Planetary Science Letters 220, 365–377.

Kim, S.T., O'Neil, J.R., 1997. Equilibrium and nonequilibrium oxygen isotope effects in synthetic carbonates. Geochimica et Cosmochimica Acta 61, 3461–3475.

Kimoto, M., 2005. Simulated change of the east Asian circulation under global warming scenario. Geophysical Research Letters 32, L16701. doi:10.1029/2005GL023383.

Kopp, R.E., Simons, F.J., Mitrovica, J.X., Maloof, A.C., Oppenheimer, M., 2009. Probabilistic assessment of sea level during the last interglacial stage. Nature 462, 863–867.

Kripalani, R.H., Oh, J.H., Chaudhari, H.S., 2007. Response of the East Asian summer monsoon to doubled atmospheric CO_2: coupled climate model simulations and projections under IPCC AR4. Theoretical and Applied Climatology 87, 1–28.

Kukla, G., 1987. Loess stratigraphy in central China. Quaternary Science Reviews 6, 191–219.

Leakey, A.D.B., 2009. Rising atmospheric carbon dioxide concentration and the future of C_4 crops for food and fuel. Proceedings of the Royal Society B 276, 2333–2343.

Lisiecki, L.E., Raymo, M.E., 2005. A Pliocene–Pleistocene stack of 57 globally distributed benthic $\delta^{18}O$ records. Paleoceanography 20, PA1003. doi:10.1029/2004PA001071.

Liu, T.S., 1985. Loess and the Environment. China Ocean Press, Beijing.

Liu, T., Ding, Z., 1998. Chinese loess and the paleomonsoon. Annual Review of Earth and Planetary Sciences 26, 111–145.

Liu, W., Huang, Y., An, Z., Clemens, S.C., Li, L., Prell, W.L., Ning, Y., 2005. Summer monsoon intensity controls C_4/C_3 plant abundance during the last 35 ka in the Chinese Loess Plateau: carbon isotope evidence from bulk organic matter and individual leaf waxes. Palaeogeography, Palaeoclimatology, Palaeoecology 220, 243–254.

Liu, Z., Tian, L., Chai, X., Yao, T., 2008. A model-based determination of spatial variation of precipitation $\delta^{18}O$ over China. Chemical Geology 249, 203–212.

Liu, S., Mo, X., Lin, Z., Xu, Y., Ji, J., Wen, G., Richey, J., 2010. Crop yield responses to climate change in the Huang-Huai-Hai Plain of China. Agricultural Water Management 97, 1195–1209.

Lu, Y.C., Wang, X.L., Wintle, A.G., 2007. A new OSL chronology for dust accumulation in the last 130,000 yr for the Chinese Loess Plateau. Quaternary Research 67, 152–160.

Lü, H., Wang, Y., Wang, G., Yang, H., Li, Z., 2000. Analysis of carbon isotope in phytoliths from C_3 and C_4 plants and modern soils. Chinese Science Bulletin 45, 1804–1808.

Noy-Meir, I., 1973. Desert ecosystems: environment and producers. Annual Review of Ecology and Systematics 4, 25–51.

O'Leary, M.H., 1988. Carbon isotopes in photosynthesis. Bioscience 38, 328–336.

Ode, D.J., Tieszen, L.L., Lerman, J.C., 1980. The seasonal contribution of C_3 and C_4 plant species to primary production in a mixed prairie. Ecology 61, 1304–1311.

Passey, B.H., Ayliffe, L.K., Kaakinen, A., Zhang, Z., Eronen, J.T., Zhu, Y., Zhou, L., Cerling, T.E., Fortelius, M., 2009. Strengthened East Asian summer monsoons during a period of high-latitude warmth? Isotopic evidence from Mio-Pliocene fossil mammals and soil carbonates from northern China. Earth and Planetary Science Letters 277, 443–452.

Quade, J., Cerling, T.E., Bowman, J.R., 1989. Systematic variations in the carbon and oxygen isotopic composition of pedogenic carbonate along elevation transects in the southern Great Basin, United States. Geological Society of America Bulletin 101, 464–475.

Quade, J., Rech, J.A., Latorre, C., Betancourt, J.L., Gleeson, E., Kalin, M.T.K., 2007. Soils at the hyperarid margin: the isotopic composition of soil carbonate from the Atacama Desert, Northern Chile. Geochimica et Cosmochimica Acta 71, 3772–3795.

Rao, Z.G., Jia, G.D., Zhu, Z.Y., Wu, Y., Zhang, J.W., 2008. Comparison of the carbon isotope composition of total organic carbon and long-chain *n*-alkanes from surface soils in eastern China and their significance. Chinese Science Bulletin 53, 3921–3927.

Reynolds, J.F., Kemp, P.R., Ogle, K., Fernández, R.J., 2004. Modifying the 'pulse–reserve' paradigm for deserts of North America: precipitation pulses, soil water, and plant responses. Oecologia 141, 194–210.

Royer, D.L., 1999. Depth to pedogenic carbonate horizon as a paleoprecipitation indicator? Geology 27, 1123–1126.

Rozanski, K., Araguás-Araguás, L., Gonfiantini, R., 1993. Isotopic patterns in modern global precipitation. In: Swart, P.K., Lohmann, K.C., McKenzie, J., Savin, S. (Eds.), Climate Change in Continental Isotopic Records. : Geophysical Monograph, 78. American Geophysical Union, Washington, D.C., pp. 1–36.

Rutter, N.W., Ding, Z.L., Evans, M.E., Liu, T.S., 1991. Baoji-type pedostratigraphic section, Loess Plateau, north-central China. Quaternary Science Reviews 10, 1–22.

Sage, R.F., Wedin, D.A., Li, M., 1999. The biogeography of C_4 photosynthesis: patterns and controlling factors. In: Sage, R.F., Monson, R.K. (Eds.), C_4 Plant Biology. Academic Press, San Diego, pp. 313–373.

Siddall, M., Chappell, J., Potter, E.-K., 2007. Eustatic sea level during past interglacials. In: Sirocko, F., Claussen, M., Sánchez Goñi, M.F., Litt, T. (Eds.), The Climate of Past Interglacials. : Developments in Quaternary Science, vol. 7. Elsevier, Amsterdam, pp. 75–92.

Still, C.J., Berry, J.A., Collatz, G.J., DeFries, R.S., 2003. Global distribution of C_3 and C_4 vegetation: carbon cycle implications. Global Biogeochemical Cycles 17, 1006. doi:10.1029/2001GB001807.

Sun, Y., Ding, Y.H., 2010. A projection of future changes in summer precipitation and monsoon in East Asia. Science China Earth Sciences 53, 284–300.
Sun, X., Song, C., Wang, F., Sun, M., 1997. Vegetation history of the Loess Plateau of China during the last 100,000 years based on pollen data. Quaternary International 37, 25–36.
Vidic, N.J., Montañez, I.P., 2004. Climatically driven glacial–interglacial variations in C_3 and C_4 plant proportions on the Chinese Loess Plateau. Geology 32, 337–340.
Vuille, M., Werner, M., Bradley, R.S., Keimig, F., 2005. Stable isotopes in precipitation in the Asian monsoon region. Journal of Geophysical Research 110, D23108. doi:10.1029/2005JD006022.
Wang, R.Z., 2003. Photosynthetic pathway and morphological functional types in the steppe vegetation from Inner Mongolia, North China. Photosynthetica 41, 143–150.
Wang, H., Follmer, L.R., 1998. Proxy of monsoon seasonality in carbon isotopes from paleosols of the southern Chinese Loess Plateau. Geology 26, 987–990.
Wang, Y., Zheng, S.H., 1989. Paleosol nodules as Pleistocene paleoclimatic indicators, Luochuan, P.R. China. Palaeogeography, Palaeoclimatology, Palaeoecology 76, 39–44.
Warne, R.W., Pershall, A.D., Wolf, B.O., 2010. Linking precipitation and C_3–C_4 plant production to resource dynamics in higher-trophic-level consumers. Ecology 91, 1628–1638.
Yang, S.L., Ding, Z.L., 2003. Color reflectance of Chinese loess and its implications for climate gradient changes during the last two glacial–interglacial cycles. Geophysical Research Letters 30, 2058. doi:10.1029/2003GL018346.
Yang, S., Ding, Z., 2008. Advance-retreat history of the East-Asian summer monsoon rainfall belt over northern China during the last two glacial–interglacial cycles. Earth and Planetary Science Letters 274, 499–510.
Yang, S., Ding, Z., 2010. Drastic climatic shift at ~2.8 Ma as recorded in eolian deposits of China and its implications for redefining the Pliocene–Pleistocene boundary. Quaternary International 219, 37–44.
Zhang, Z., Zhao, M., Lu, H., Faiia, A.M., 2003. Lower temperature as the main cause of C_4 plant declines during the glacial periods on the Chinese Loess Plateau. Earth and Planetary Science Letters 214, 467–481.